Gas transfer velocities in small forested ponds

Towards an understanding of carbon cycling in small inland waters

Emily Farr

Advisor: Peter Raymond

Second Reader: Hagit Affek

4/27/14

A Senior Thesis presented to the faculty of the Department of Geology and Geophysics, Yale University, in partial fulfillment of the Bachelor's Degree.

Abstract

Inland waters process substantial amounts of carbon relative to their small surface area, and may play a significant role in regional and global carbon budgets. In order to quantify the amount of carbon inland waters release to the atmosphere, accurate estimates of air-water gas exchange rates are needed. Gas exchange is controlled by the gas concentration differential between the air and water and turbulence at the water's surface, which in lakes and ponds is primarily regulated by wind and convection. A significant body of research exists on the relationship between wind and gas exchange in large systems, but little is known about the processes regulating gas transfer and carbon dynamics in small systems. In this study, we determined the gas transfer velocity coefficient, k_{600}, in four small (< 250 m^2), low-wind (< 2 m s^{-1}) vernal pools using a direct gas injection of propane. We measured the loss of propane over 96 hours and then calculated k_{600} for each 12-hour sampling interval. The overall k_{600} for the four ponds was 0.36 ± 0.08 m day^{-1}. We evaluated the role of wind speed, convection, and rain on gas exchange. Wind speed was not able to independently predict k_{600}, and convection dominated over wind in determining turbulence during all periods with net pond cooling. Rain was not found to have a significant impact on k_{600}. Our study shows that the gas transfer velocities in small inland ponds are lower than those observed in larger bodies of water with higher wind speeds, and are in agreement with the surface area-k_{600} relationship seen in previous studies.

Contents

1 Introduction

Lakes, streams, and ponds play an active role in carbon budgets through both the sequestration and efflux of CO_2 and CH_4 greenhouse gases (Raymond et al. 2013, Cole et al. 2007). These inland waters are numerically dominated by water bodies smaller than 1 km^2 (Downing et al. 2006), which suggests that small lakes and ponds may play a globally significant role in processes such as carbon cycling. Small ponds serve as a locus for the collection and export of terrestrial carbon to the atmosphere, and have higher concentrations of CO_2 (Kelly et al. 2001) and higher CO_2 flux into the atmosphere per unit area than do most lakes and reservoirs (Torgerson and Branco 2008). The estimated net global contribution of small (< 0.01 km^2), shallow ponds to the carbon cycle is 0.25-2.5 x 10^{14} g C a^{-1}, which is on the order of carbon fluxes from lakes and rivers as well as the net terrestrial carbon uptake (Torgerson and Branco 2008).

Understanding the biogeochemical cycling of carbon in inland waters requires an accurate measurement of the air-water gas exchange coefficient, *k* (Raymond et al. 2012), which is used to calculate the exchange rate of gases between the atmosphere and a body of water. Determination of gas transfer velocities is useful in many contexts, in particular for studies of ecosystem metabolism and the role of various water bodies in the regional or global carbon cycle (Cole et al. 2010).

Wind speed is the main driver of gas exchange in high wind systems, creating turbulence through surface waves and shear stress (MacInytre et al. 1995). Fetch, the distance wind travels across a body of water, also affects gas transfer velocity and varies with the size and local geometry of the body of water as well as the wind speed (Wanninkhof 1992). Larger bodies of water with higher fetch allow the development of larger surface waves from wind, which generate turbulence. Accordingly, *k* tends to be larger in larger lakes (Read et al. 2012). Many studies have determined fetch and surface area to be the most important contributors to energy transfer at the surface of lakes (Markfort et al. 2010). At low wind speeds, the lack of a general relationship with gas exchange rate suggests that other factors dominate.

Other parameters influencing turbulence and thus gas exchange include rain, convection, and water chemistry. Rainfall can significantly influence the gas exchange rate both from increased turbulence and the rain dilution effect, which alters the differential partial pressure gradient between the air and water by changing the gas concentration (Ho et al. 1997). Seasonal

temperature variations and diurnal thermal convection influence *k*, particularly in wetlands and small bodies of water (Poindexter and Variano 2013; Matthews et al. 2003). Convection from cooling surface waters has been demonstrated to increase gas transfer velocities in low to moderate wind systems by increasing turbulence in the surface mixing layer (SML) (MacIntyre et al. 2010). Surface area regulates the relative importance of convection and wind shear in influencing *k*, with wind shear often dominating in larger systems and convection playing a larger role in small lakes and ponds (Read et al. 2012). Local water chemistry also enhances the gas transfer velocity in a number of ways including the formation of surface films and chemical enhancement. Surface films, formed by hydrophobic organic compounds, reduce the wind stress at the surface and may alter the Schmidt number dependence of the gas by physically obstructing molecular diffusion (MacIntyre et al. 1995), therefore decreasing the gas transfer velocity. All of these play a role in determining the *k* for each body of water, with different factors dominating based on the local environment.

Many lake experiments have estimated *k* with predictive models using wind speed (e.g., Cole and Caraco, 1998, Wanninkhof 1992, Clark et al. 1994) and a surface renewal model based on wind speed and buoyancy flux (e.g., Read et al. 2012, MacIntyre et al. 2010). These models show a correlation between wind speed and *k* at moderate-to-high wind speeds, but most have determined that the relationship breaks down at low wind speeds (wind speed (U) < 3 m s^{-1}) (e.g., Clark et al. 1994; Cole et al. 2010; Wanninkhof 1992). Consequently, the large variation in wind speeds, size and geometry of water bodies, and other ecosystem parameters merits direct measurement of the gas exchange coefficient (Wanninkhof et al. 1987), particularly in small water bodies with low wind.

Direct measurement of *k* has been performed in many aquatic ecosystems using the direct gas tracer injection method, often with SF_6, ^3He (e.g., Clark et al. 1994; Wanninkhof et al. 1985), or C_3H_8 (Jin 2008). Using this method, the gas is injected into the surface water and the flux and concentration gradient are determined by measuring the decline in concentration over a period of days or weeks, depending on the size of the body of water. Ideal tracer gases are biological and chemically nonreactive, have very small background concentrations in the natural waters, and can be detected at low concentrations (Clark et al. 1994). Most previous experiments with direct measurement of gas transfer velocities have been performed in large bodies of water at moderate

wind speeds. Little data exists for small, protected lakes and ponds, and the mechanisms that control gas transfer at low wind speeds are not well understood (Crusius and Wanninkhof 2003).

In this study, we measured the gas transfer velocity, *k*, in four small (< 250 m^2), low-wind ($U < 2$ m s^{-1}) ponds using direct propane injections. We also compared gas exchange rates to environmental influences including wind speed, convection, and rain. We expected to find low values of *k* as a result of the small surface area and low wind, and a dominance of convection over wind speed in determining *k*.

1.1 Ecosystem Background

Vernal pools are abundant on the landscape, with one to ten ponds per square kilometer of undeveloped land in the northeastern United States (Brooks 2005). The ponds form in the fall and dry up by late summer, freezing over in the winter months. Like many aquatic systems, these vernal pools are net heterotrophic (Atwood 2012), meaning they produce more carbon dioxide (CO_2) than they consume. Carbon cycling in vernal pools could be significant partly because of the high annual input of leaf litter they receive from the surrounding terrestrial forest, adding large amounts of carbon to the system. Unlike in lake and river ecosystems where carbon inputs are diluted or transported downstream, vernal pools are small and stationary, making them ideal for an analysis of the carbon cycling related to leaf litter inputs. Upon entering these ponds, leaf litter is broken down through microbial decomposition, a process that produces CO_2 and consumes oxygen. This decomposition leads to seasonal anoxic conditions in vernal pools through its consumption of oxygen. When oxygen is depleted, methanogenic and methanotrophic bacteria, a different kind of microbial decomposer, begin to produce and consume methane, a gas that has twenty-five times the warming potential of CO_2 (Bridgham et al. 2013). Research suggests that methane (CH_4) emissions from wetlands make up around 25% of all methane released into the atmosphere (Whalen 2005). Consequently, small ponds often have high concentrations of CO_2 and CH_4 (Kelly et al. 2001), which are both important greenhouse gases. Despite the abundance of small ponds on the landscape, small inland waters are rarely accounted for in global carbon budgets and merit further investigation.

2 Methods

2.1 Study Sites

We evaluated the gas exchange coefficient, *k*, in four small, temporary ponds in Yale-Myers forest located in northeastern Connecticut during May and June of 2013 (Figure 1). The ponds range in surface area from 181 to 225 m^2 and in mean depth from 41 to 56 cm (Table 1). All four ponds, Westford, Brookside, CH, and RH, were chosen for their closed basins with minimal emergent vegetation. The closed basin prevents gas tracer dilution from inflow as well as escape to reservoirs other than the atmosphere. The lack of emergent vegetation ensured that plant matter was not altering the rate of exchange. During its sampling period, RH had ferns in about 20% of the basin along the edge and about 10 trees in the sides of the basin because it was sampled after a period of rain and higher water levels. The ponds are heavily sheltered by the surrounding forest and thus have negligible fetch.

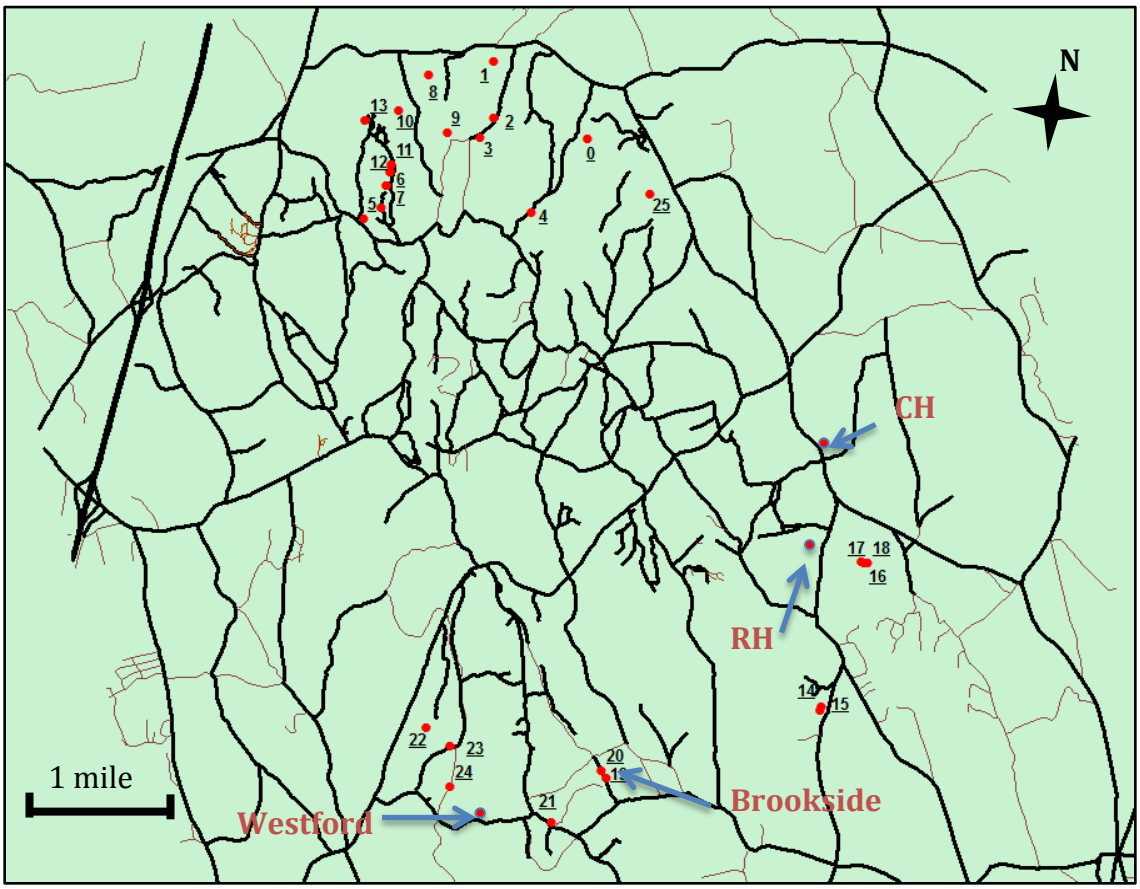

Figure 1: Subset of vernal pools in Yale-Myers forest mapped by the 2012 forest crew. Red dots signify ponds, lines denote main roads, and brown lines denote forest or logging roads. Ponds utilized in this experiment are labeled. Scale is approximated.

Table 1. Surface area and average depth measurements for each pond

Pond	Surface Area (m^2)	Avg. Depth (cm)	Max. Depth (cm)
Westford	213	41	95
Brookside	225	46	71
CH	181	48	69
RH	197	56	117

2.2 Theory of Gas Exchange

Gas transfer between aquatic surfaces and the atmosphere can be described by the equation:

$$F = k(C_{sur}\text{-}C_{eq}) \quad (1)$$

where F is the gas flux in flow rate per unit time, k is the piston velocity or gas exchange coefficient with a unit of length per unit time, C_{sur} is the concentration of the gas in question in the surface water, and C_{eq} is the atmospheric equilibrium concentration of the gas (e.g., Cole et al. 2010). Gas transfer is regulated primarily by two parameters. The first is the differential partial pressure gradient between the air and water (Cole et al. 2010), which can be easily measured and is represented by C_{sur} - C_{eq}, causing gas transfer through molecular diffusion across the air-water interface. The second is the turbulence at the air-water interface, which is controlled by numerous factors including wind, rain, and differential heating (e.g., Jähne et al. 1987, Macintyre et al. 1995, Clark et al. 1994), and is described by the gas transfer coefficient k. Though k is a function of many complex turbulence parameters, it is possible to directly measure F, C_{sur}, and C_{eq} in order to derive k.

In the uppermost part of the aquatic boundary layer, molecular diffusion caused by the differential partial pressure gradient between air and water dominates the process of gas transfer. This molecular diffusion can be described by the Schmidt number (Sc), which is defined as the ratio between the kinematic viscosity of water, v, and the diffusion coefficient of the gas, D (Jähne et al. 1987):

$$Sc = v/D \quad (2)$$

At a smooth surface with no turbulence, gas transfer velocity depends solely on Sc (Jähne et al. 1987). Consequently, gas-specific Schmidt numbers can be used to constrain the variation in air-

water gas exchange for different gases. The Schmidt number (2) is used to determine the *k* value for one gas at a given temperature, which can then be used to calculate *k* values for other gases and temperatures. Most analyses of gas transfer velocity normalize *k* to a value of k_{600} for comparison between gases. k_{600} is the *k* for CO_2 at 20°C and corresponds to a Schmidt number of 600, which can be related to the *k* for any other gas using the equation (Wanninkhof et al. 1987):

$$\frac{k_{600}}{k_{gas2}} = \left(\frac{600}{Sc_{gas2}}\right)^{n} \quad (3)$$

where *Sc* denotes the Schmidt number for the particular gas of interest, and *n* is the Schmidt exponent which varies from -0.5 to -0.67 depending on the boundary conditions. In low-wind environments (< 3 m s^{-1}), *n* can be assumed to equal -0.67 (Matthews et al. 2003; Jähne et al. 1987).

2.2 Field Methods

2.2.1 Datalogger & Bathymetry

We used a datalogger (Campbell Scientific CR300) to measure wind speed (m s^{-1}) and wind direction (degrees), air and water temperature (°C), PAR (photosynthetically active radiation) (μmol s^{-1} m^{-2}), and rainfall (mm) at 15-minute intervals throughout the course of each pond experiment (Figure 2). We positioned the anemometer (height above water level: Westford 75 cm, Brookside 77 cm, CH 50 cm, RH 35 cm), temperature probes, and photometer (LI-190 Quantum Sensor, LI-COR) on a stake at the deepest point of each pond. We positioned the water temperature probe approximately 7 cm below each pond surface. A tipping-bucket rain gauge located on a separate stake in the least canopy-covered region of each basin measured the total rain (mm) in each interval. We determined the bathymetry of each pond by measuring depth every meter along five transects per pond. We assumed ponds had elliptical basins and used these depth measurements to estimate pond volume and surface area.

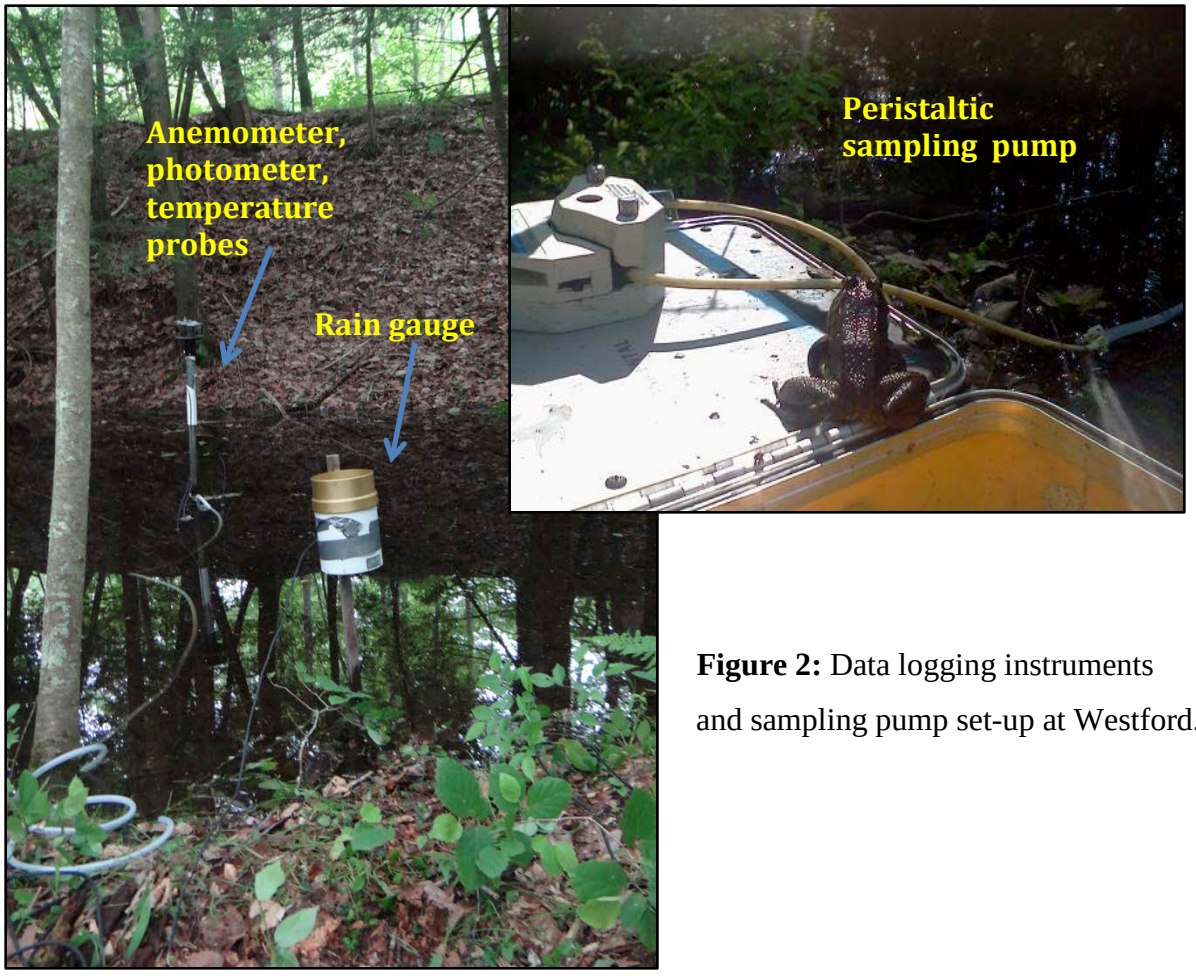

Figure 2: Data logging instruments and sampling pump set-up at Westford.

2.2.2 Propane Injection

Propane was selected for direct injection because it is an inert gas with negligible background concentrations in the air and water. The propane release experiment was performed in each pond over separate 5-day periods. On the first day of sampling, we bubbled propane into eight 18.9-L carboys filled with pond water for 10 minutes each at 13 psi using an airstone. We added 3 ml of rhodamine to each carboy as a tracer to easily determine when the pond had completely mixed. The carboys were well mixed and we sampled each carboy to determine initial propane concentrations. We then poured the carboy mixtures into the pond, making sure to distribute them around the entire pond basin. We used a handheld datalogger (Turner Designs DataBank^{TM}) to measure rhodamine concentrations twice a day for the first two days to verify that the propane concentration mixed homogeneously throughout the pond.

2.2.3 Propane gas sampling

We measured propane concentrations in each pond over a 96-hour period. We took our first measurements six hours after the propane addition, which is when rhodamine concentrations indicated that the propane had mixed evenly throughout the pond basin. We measured propane concentrations from surface waters (approximately 13 cm below the surface) at the deepest point of each pond using a peristaltic pump (Cole-Parmer Masterflex E/S^{TM} portable sampler, 115 VAC) between the hours of 8 a.m. and 8 p.m. due to daylight constraints. We took samples every 2 hours for the first 24 hours, then at 3-hour intervals for the remaining 72 hours (Table 2). We measured propane concentrations using a headspace equilibrium technique (Raymond et al. 1997). Briefly, we filled a beaker with water from the peristaltic pump and allowed it to flush for several volumes in order to obtain a representative water sample. We ran the pump continuously during sampling in order to avoid outgassing of propane from the beaker in between measurements. We took three replicate water samples by drawing 40 ml of water from the beaker into a 60-ml syringe with a three-way Luer taper, then immediately drawing in 20 ml of ambient air. The Luer taper was rotated to seal the syringe, which was then shaken for 2 minutes in order to equilibrate the propane concentration between the water and the headspace, transferring nearly all of the insoluble propane into the gas phase. A 20-ml syringe was then used to draw in 15 ml of the headspace gas. A needle was attached to the 20-ml syringe and the 15 ml of gas was injected into an airtight, evacuated glass vial (Labco Limited, United Kingdom).

Table 2. Brookside pond sampling schedule, representative of all 4 ponds.

Date	**Hours Sampled**
11-June-2013	14:00, 16:00, 18:00, 20:00
12-June-2013	8:00, 10:00, 12:00, 14:00, 17:00, 20:00
13-June-2013	8:00, 11:00, 14:00, 17:00, 20:00
14-June-2013	8:00, 11:00, 14:00, 17:00, 20:00
15-June-2013	8:00, 11:00, 14:00

2.2.4 Sources of Sampling Error

The sampling pump used for propane gas samples was not fully functional throughout the course of the experiment, which may have contributed to some inconsistencies in the propane concentration data. The pump was broken on the fifth day of sampling in Westford (01 June 2013), for the entire sampling period in Brookside (11 June 2013 – 15 June 2013), and for the final day of sampling in RH (29 June 2013). During these days, we obtained gas samples by wading a few feet into the ponds. This disturbance of the water may have locally enhanced the gas exchange, leading to potential error in the slope of gas release into the atmosphere.

Additionally, since the canopy heavily sheltered the ponds from rain events, the stationary rain gauge measurements may not be indicative of the rain over the entire surface area.

2.3 Propane Lab Analysis

We measured propane concentrations in each of the gas samples using a gas chromatograph (GC) (SRI 310C) with a 3.5-mm column. PeakSimple 4.09 software calculated propane peak area in each sample, using 95% peak sensitivity and 60% baseline sensitivity. We calibrated the GC for propane using Airgas propane standards of 1000 ppm_v and 50 ppm_v to construct a linear regression and determine the propane peak area to concentration (ppm_v) ratio. The propane sample analysis temperature settings were as follows: detector temperature to 150°C and oven temperature to 100°C, resulting in a propane retention time of ~4.08 minutes. We injected all propane samples in 1-ml quantities into the GC injection port with a 1-ml syringe. After the propane had fully exited the column at ~5.75 minutes, we ramped up the over temperature to 200°C for ~3.3 minutes to clear out any remaining gases in the sample. We also ran propane samples taken from the eight carboys for each pond on the GC with equivalent initial temperature settings but injected 0.5-ml volumes. We converted propane peak areas to ppm_v using the calibration curves.

2.4 Calculation of *k*

We used a Grubbs outlier test to discount any erroneous propane concentrations that resulted from sampling error. We converted the average propane concentrations (ppm_v) of the triplicates at each time point to units of mol L^{-1} using Henry's law constants (Mohebbi et al. 2012). We calculated *k* values for each 12-hour sampling interval because longer time scales

more accurately reflect the overall ecosystem gas transfer velocity by decreasing error (Wanninkhof 1987). We calculated *k* for the first day of sampling in each pond over a 6-hour interval because propane sampling occurred from 2 p.m. to 8 p.m. on those days.

We calculated daily and nightly *k* (m day^{-1}) using the following equation (Wanninkhof et al. 1987):

$$k = \frac{h}{\Delta t}\ ln\frac{C_i - C_o}{C_f - C_o} \tag{4}$$

where *h* is the average depth of the pond in m, Δt is the time interval in days, C_i and C_f are the initial and final propane concentrations in the pond, respectively, and C_o is the background concentration of propane in the water. We computed average pond depth, *h*, by taking the mean of the measured depths for each square meter measured in each pond. Since C_o of propane is negligible in this experiment, (4) becomes (Wanninkhof et al. 1987):

$$k = \frac{h}{\Delta t}\ ln\frac{C_i}{C_f} \tag{5}$$

In this experiment, we took multiple gas samples between C_i and C_f for each day, where Δt between the initial and final concentration is 12-hours, or half a day. Consequently, we performed a simple linear regression to determine the slope of concentration change over time for each 12-hour daytime interval of sampling, and this slope replaced $\frac{1}{\Delta t}\ ln\frac{C_i}{C_f}$ in (5). We did not take any gas samples between 8 p.m. and 8 a.m. during the experiment, so we calculated the *k* values for each night of sampling using C_f from the previous day as the initial propane concentration and C_i from the following day as the final propane concentration. After calculation using (5) and the regression slope, we normalized *k* values to a k_{600} to allow comparison with other gases (Cole at al 2010) using (3). We assumed the Schmidt exponent *n* to equal -0.67 because nearly all measured wind speeds were below 3 m s^{-1} (Jähne et al. 1987).

2.5 Analysis of Environmental Parameters

In order to evaluate if k_{600} was influenced by environmental and pond-specific variables, we used multiple linear regression of k_{600} versus average wind speed, rain, surface area, average depth, light flux, and diurnal temperature change (See Appendix B). To normalize the measured average wind speed over each 12-hour interval to a measurement height of 10 m, we assumed a logarithmic wind profile and a neutrally stable boundary layer (Clark et al. 1994), and a surface roughness of 0.01 m^{-1} (Markfort et al. 2010). We created a variable for rain by indicating values

of k_{600} that occurred within 12 hours after rainfall events greater than 10 mm. We removed insignificant variables in the multiple linear regression model individually until all predictors were significant ($p < 0.05$). We then analyzed the correlation between significant predictors and k_{600} independently in order to determine whether any predictive relationship could be found.

2.6 Calculation of u^*/w^*

We determined the relative importance of convection and wind to turbulence in the ponds by calculating the ratio between the velocity scales for wind shear (u^*) and for convection (w^*) in the SML (sensu Read et al. 2012). This ratio is a proxy that is used to compare the contribution of wind and heat loss to turbulent kinetic energy in the SML (Read et al. 2012).

We calculated w^* using the following equation (Read et al. 2012):

$$w* = (-\beta z_{mix})^{1/3} \quad (6)$$

where β is the buoyancy flux in $m^2\ s^{-3}$, and z_{mix} is the average depth of the pond in m. We assumed the four ponds used in this experiment were well mixed throughout, so the average depth of each pond represents the SML. Buoyancy flux is defined as (Read et al. 2012):

$$\beta = {g\alpha H*}/{C_p\rho_w} \quad (7)$$

where g is the acceleration due to gravity, α is the coefficient of thermal expansion assumed to equal $69*10^{-6}\ K^{-1}$, H^* is the effective surface heat flux in W m^{-2}, C_p is the specific heat of water, and ρ_w is the density of water. A negative buoyancy flux indicates a net loss of energy from the surface water, which signals the presence of convection. A positive buoyancy flux indicates increased temperature stratification of the surface water, primarily caused by the influx of solar radiation, so we set w^* to 0 when $\beta > 0$ (Read et al. 2012). The surface heat flux (H^*) is defined as (Read et al. 2012):

$$H* = Q_S - R_0\left[\left(2 - 2\exp(-z_{mix}K_d)\right)/\left(z_{mix}\,K_d - exp(-z_{mix}K_d)\right)\right] \quad (8)$$

where Q_s is the net surface energy flux, in W m^{-2}, R_0 is the measured PAR in W m^{-2}, and K_d is the light attenuation coefficient in m^{-1}. We calculated Q_s, which is the driver for buoyancy flux, using the water temperature measurements taken at 15-minute intervals throughout the pond using the equation (Poindexter and Variano 2013):

$$Q_s = C_p\rho_w z_{mix}\,{dT}/{dt} \quad (9)$$

where *dT/dt* is the rate of change of temperature over each 12-hour interval (day and night), calculated from a linear regression of the 15-minute interval temperature readings. Given the small size of the ponds, temperature was assumed to be consistent throughout. We calculated R_0 using the average PAR in each 12-hour interval. We estimated K_d using forty tabulated light attenuation values for lakes (Read et al. 2012), excluding two outliers outside the interquartile range. We created a 95% confidence interval for the K_d values, and the upper and lower bounds of this interval created a maximum error of 7% in the buoyancy flux calculations for this study. Therefore, we used the average K_d of 1.40 m^{-1} for further calculations.

To calculate $u*$, we first normalized the measured average wind speed over each 12-hour interval to a measurement height of 10 m. We assumed a logarithmic wind profile and a neutrally stable boundary layer with equations (Clark et al. 1994):

$$U_z = (u*/k) ln(z/z_0) \tag{10}$$

and

$$u* = \sqrt{C_d} U_{10} \tag{11}$$

where U_z is the wind speed measured at height z in m s^{-1}, k is the Von Karmen constant equal to 0.4, z is the height of the anemometer in m, z_o is the surface roughness in m^{-1} , C_d is the dimensionless drag coefficient, and U_{10} is the wind speed corrected to a height of 10 m. We assumed z_0 to be 0.01 m^{-1} based on the value for a smooth surface of water (Markfort et al. 2010). We determined the drag coefficient (C_d) using the following empirical model for wind speeds < 4 m s^{-1} in sheltered ponds measured at 10 m (Markfort et al. 2010):

$$C_{d,10} = 0.0044 {U_{10}}^{-1.15} \tag{12}$$

Combining equations (10)-(12) yields the equation used to normalize wind measurements to a height of 10 m:

$$U_{10} = \left(\frac{0.4 U_z}{ln(z/0.01)\sqrt{0.004}} \right)^{2.35} \tag{13}$$

We determined that scaling of wind speed based on canopy sheltering (Markfort et al. 2010) was not necessary for the four ponds in this study. Although the ponds are heavily sheltered by the surrounding canopy, the ratio of pond size to canopy height is such that the wind speed at the surface is functionally unrelated to the wind speed above the canopy. The ponds are not large enough for fetch to play a significant role in wind development over the surface of the water, so we assumed the wind speed to be equal over the entire surface of the pond. Since we took wind

speed measurements near the surface of the water, we used the values of U_{10} directly calculated from these measurements to calculate $u*$.

We calculated $u*$ using the equation (Read et al. 2012):

$$u* = \left(\tau_0/\rho_w\right)^{1/2} \quad (14)$$

where

$$\tau_0 = C_d {U_{10}}^2 \rho_a \quad (15)$$

and ρ_a is defined as the density of air calculated using the average 12-hour air temperature measurements.

The velocity scales for $u*$ and $w*$ were calculated for each 12-hour interval of sampling. When $u*/w* = 0.75$, convection and wind contribute equally, and any value below 0.75 indicates that convection plays a larger role than wind shear in surface turbulence.

3 Results

3.1 Gas transfer velocity, k_{600}

Surface water propane concentrations decreased exponentially over the sampling period in all four ponds (Figure 3), indicating continuous propane evasion from the ponds to the atmosphere. Initial concentrations of propane measured in the ponds ranged from 114 nmol L^{-1} in CH to 317 nmol L^{1} in Westford (Table 3), and decreased between 50 and 93% during the 96-hour sampling periods.

Table 3: Surface water propane concentrations over sampling period for the four ponds.

Pond	Initial concentration (nmol L^{-1})	Final concentration (nmol L^{-1}) 94-96 hours after release	Percent decrease
Westford	317	38.0	88
Brookside	161	11.9	93
CH	114	57.3	50
RH	122	26.9	78

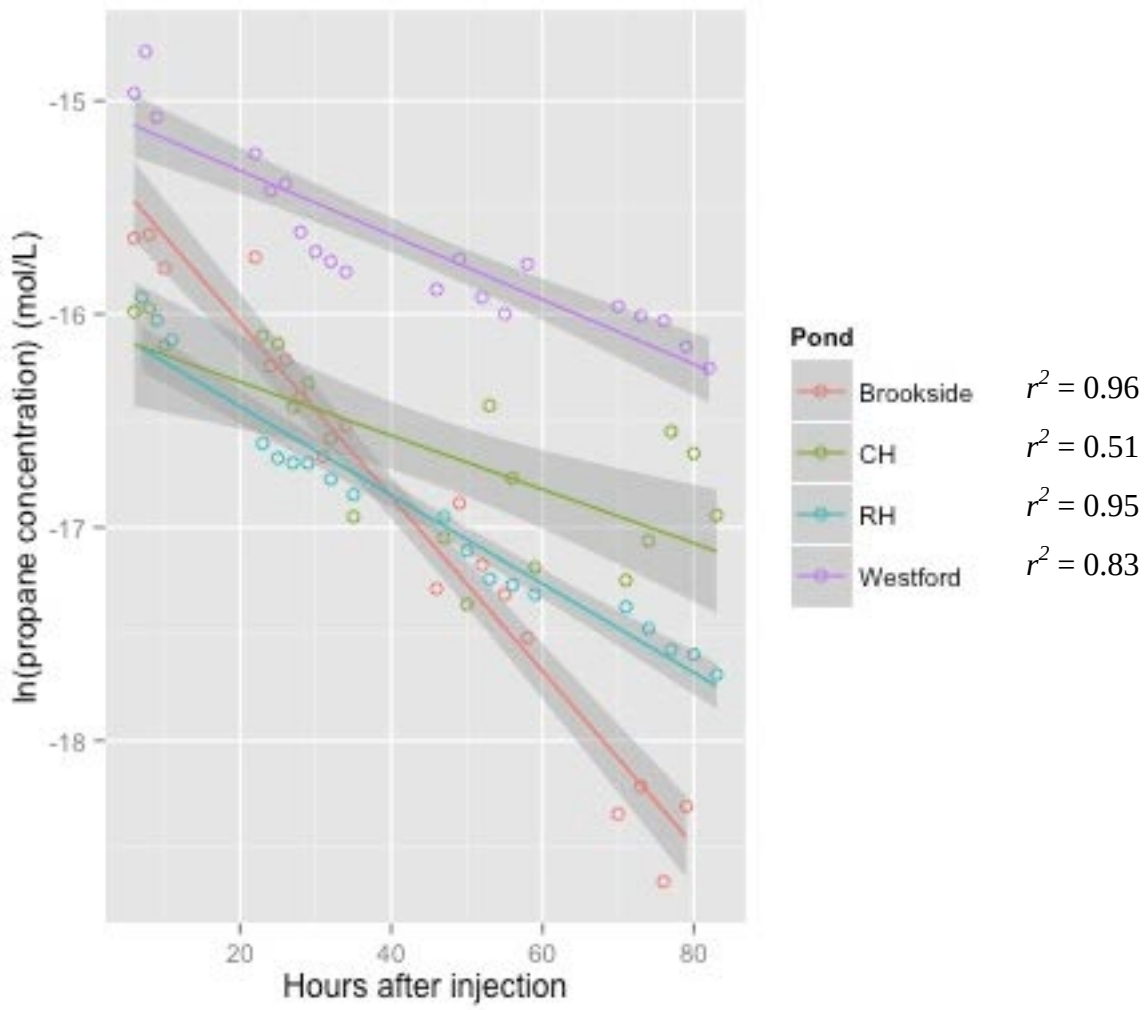

Figure 3: Surface water propane concentrations over sampling period of each pond.

The average k_{600} across all ponds was 0.36 ± 0.08 m day^{-1} (1 standard error). The k_{600} values for day 5 of each pond's sampling period were discarded because propane concentrations had reached < 30 ppm_v. Concentrations near the detection limit can lead to erroneous calculations (Genereux and Hemond 1992), and led to negative values of k_{600} in this study. Although the k_{600} value for the fourth night of sampling in each pond was calculated utilizing the first gas sample for the fifth day of sampling, those values of k_{600} were not determined to be significantly different from the other overnight k_{600} values (t-test, t = -1.71, df = 16.42, p = 0.11) and were thus included in the analysis.

The average k_{600} was 0.48 ± 0.12 m day^{-1} during the day and 0.24 ± 0.09 m day^{-1} (1 standard error) at night (Figure 4), but this difference was not statistically significant (t-test, t = 1.60, df = 27.93, p = 0.12). Gas transfer velocity did not differ significantly between ponds (ANOVA, *f-value* = 1.50, df = 3, p = 0.24) but did range from an average k_{600} of 0.12 m day^{-1} in CH to 0.52 m day^{-1} in Brookside (Table 4, Figure 5). The analysis of the relationship between environmental and pond variables and k_{600} revealed that average wind speed ($U_{10,\,avg}$), rain, depth, and surface area were all significant predictors for k_{600} (multiple linear regression, df = 27, all $p < 0.05$, adjusted r^2 = 0.27), and together explain 27% of the variability in gas transfer velocity. Other factors of daily light flux and diurnal temperature change were not significantly correlated with k_{600} (multiple linear regression, all $p > 0.1$). Neither the environmental variables of $U_{10,avg}$ (simple linear regression, df = 30, p = 0.10, r^2 = 0.09) and rain (simple linear regression, df = 30, p = 0.34, r^2 = 0.03) nor pond-specific variables of surface area (ANOVA, *f-value* = 2.19, df = 1, p = 0.15) and pond depth (ANOVA, *f-value* = 0.36, df = 1, p = 0.56) have a predictive relationship with k_{600} when analyzed independently.

Table 4: Summary of pond-specific measurements, including k_{600} averaged over each pond and overall k_{600} calculated over the full sampling period (94-96 hour) in each pond.

Pond	Westford	Brookside	CH	RH
k_{600}, Avg. 12-hr (m day^{-1})	0.31	0.52	0.12	0.49
k_{600}, Full Sampling Pd. (m day^{-1})	0.18	0.71	0.02	0.44
Avg. Water Temperature (°C)	15.32	15.27	16.09	15.93
Avg. Measured Wind Speed (m s^{-1})	0.33	0.30	0.34	0.35
Avg. U_{10}, Wind Speed at 10 m (m s^{-1})	0.34	0.25	0.30	0.15
Max. Measured Wind Speed (m s^{-1})	3.05	2.36	4.30	3.55
Total Rain (mm)	13.21	48.01	37.34	7.62

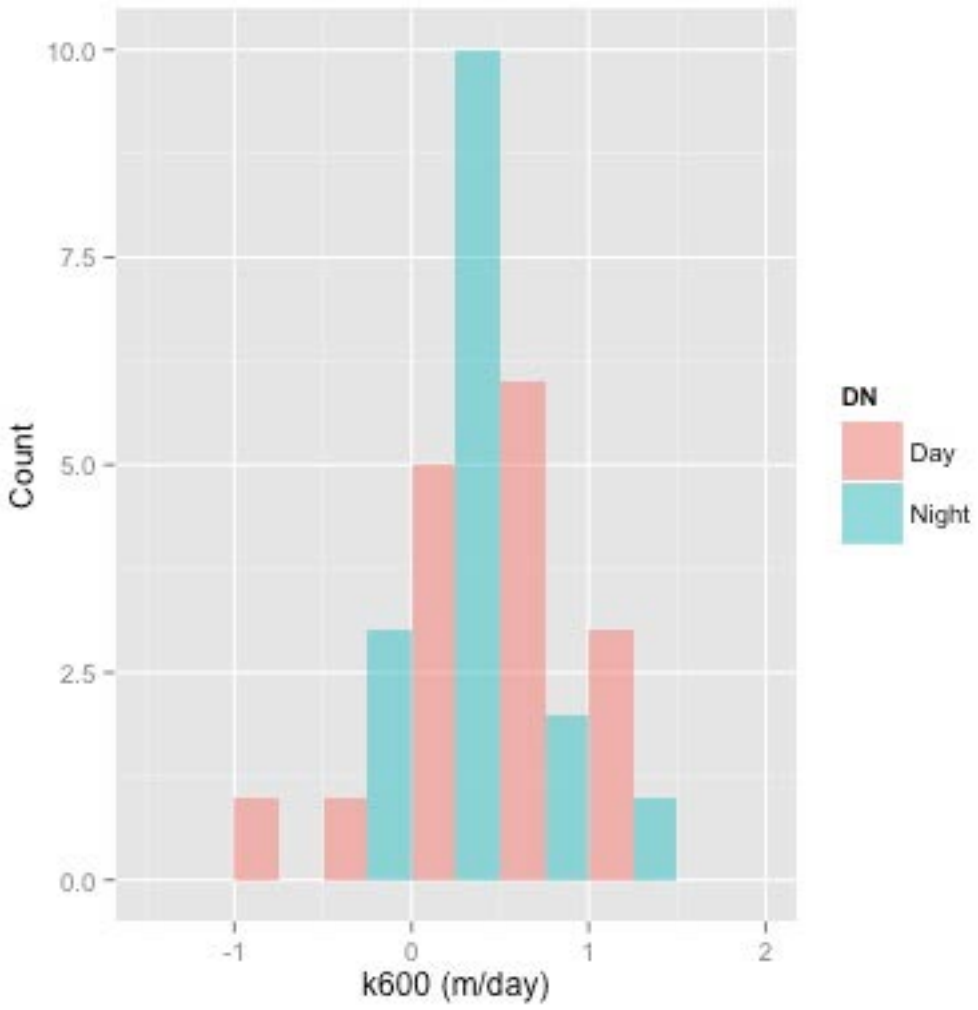

Figure 4: Histogram of k_{600} values during the day (n=16) and at night (n=16). Includes all four ponds.

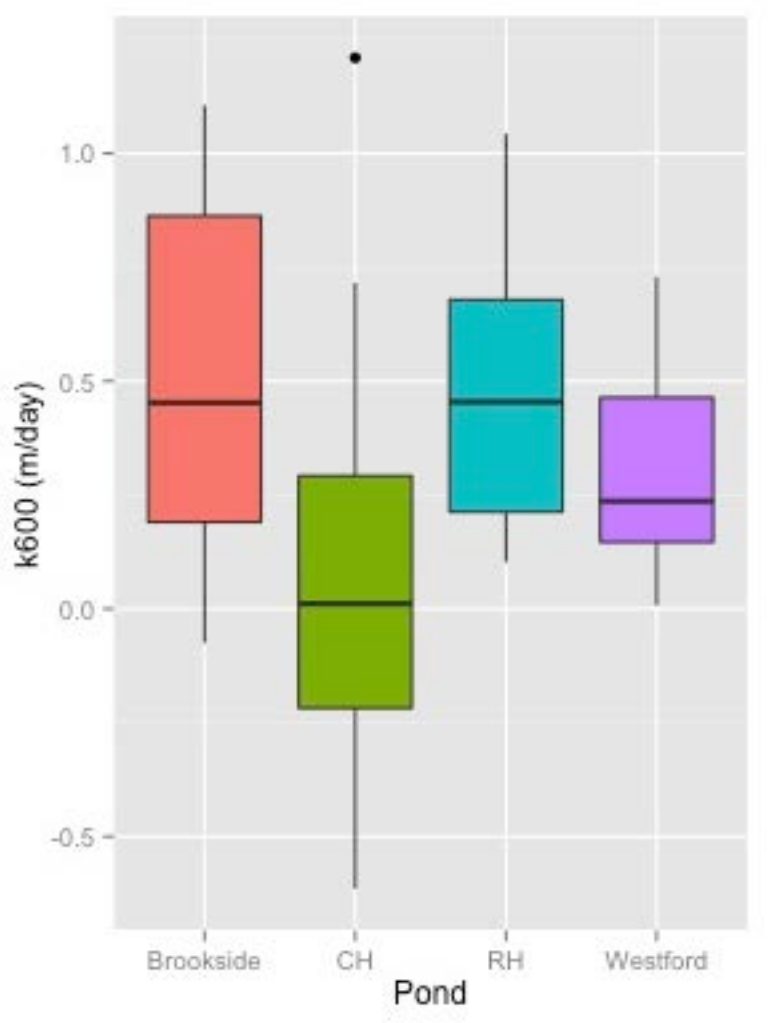

Figure 5: Gas transfer velocities (k_{600}, m day^{-1}) for the four ponds.

3.2 Relative importance of wind shear and convection, u^*/w^*

On days and nights when w^* was positive (water cooled over the 12-hour interval), convection always dominated over wind shear in terms of contribution to turbulence, with $u^*/w^* < 0.75$ in all cases (Table 5). We found no significant difference between k_{600} when $w^* = 0$ versus when $w^* > 0$ (t-test, $t = 0.48$, df = 29.93, $p = 0.63$), indicating that pond heating versus cooling did not significantly impact the k_{600}. This means that, although convection dominates over wind speed whenever the pond is cooling, there is no significant difference between k_{600} when convection is present versus when it is not. We also analyzed the difference in k_{600} during periods of heating and cooling on the finer time scale between each propane sample (2-3 hours), which was also found to not be significant (t-test, $t = -1.15$, df = 67.91, $p = 0.15$).

Table 5: The ratio of average 12-hour u^* to average 12-hour w^* for each pond, dimensionless.

Pond	Westford	Brookside	CH	RH
Average u^*/w^*	0.26	0.06	0.08	0.09

4 Discussion

This analysis used a direct propane injection to determine the gas transfer velocities in four small vernal pools. These results are important for quantification of biogeochemical cycling in inland ponds and wetlands, particularly in regards to the carbon cycle. Small ponds are abundant and serve as "hot spots" in the aquatic processing of terrestrial carbon and its export to the atmosphere (Torgersen and Branco 2008), and have been overlooked in the existing literature. Previous studies have performed direct gas tracer injections in larger lake systems, but this is the first to investigate the process of gas exchange in small (< 250 m^2) ponds. As small ponds are low in terms of both surface area and wind speed, current models of gas exchange based on wind speed or area may not apply. Though measurements in each of the ponds in this study were made on different dates, gas transfer velocities among the four ponds are comparable because environmental conditions (e.g., wind and rain) were similar throughout all sampling periods. The k_{600} observations in this study are overall slightly less than the gas transfer velocities in some of the smallest systems (566-27000 m^2) in existing literature with comparable low wind speeds (Table 6).

Table 6: k_{600} (with one standard deviation, when provided), Wind speed, surface area, and sampling method from previous studies of gas transfer velocity in individual small lakes. Data from this study is averaged over all four ponds.

Author	k_{600} (m day^{-1})	Surface Area of Studied Lake (m^2)	Wind (m s^{-1})	Method
Read et al. 2012	0.46	566	0.79	Surface renewal model
Cole et al. 2010	0.53 ± 0.09	3000	< 3.0	Floating chamber
Cole et al. 2010	0.49 ± 0.004	27000	1.28	SF_6 gas injection
This study	0.36 ± 0.43	204	0.33	Propane gas injection

Measured parameters of surface area, depth, rain quantity, light flux, and diurnal temperature change cannot independently or completely explain the differences in k_{600} within in this study. Ponds were selected primarily based on their closed basins and lack of emergent vegetation, which limited possible study sites but allowed comparison between ponds. Consequently, all four ponds studied had similar surface areas and depths, and the minor differences between the ponds were not significantly related to variations in $k_{600.}$ Though a few rain events occurred during the sampling period, rainfall did not correlate with $k_{600.}$ A few of the highest observed gas transfer velocities occurred in the 12-hour period after incidents of rain (e.g. k_{600} = 3.29 m day^{-1} on the day of 6/14 after an overnight rainfall of 29.72 mm), but this trend was not consistent. In a study of the effect of rain on gas transfer, rainfall events with < 25 mm h^{-1} were considered to be light rain (Ho et al. 1996). In this study, all rain events were < 13 mm h^{-1}, which likely contributed to the low correlation with gas transfer velocity. Since rain events were all small, the lack of variability in rainfall between days likely contributed to the low correlation with k_{600}. Diurnal temperature in each pond throughout the full sampling period of June was not significant as a result of the minimal overnight cooling that occurred during the summer months.

Turbulence at the surface of the water is a major driver of gas transfer and is controlled primarily by a balance between solar radiation, which increases stratification and decreases turbulence, and wind speed and heat loss, which create convection and destabilization of the

SML (Read et al. 2010). We were interested in the drivers of gas transfer in low-wind environments, specifically the role of convection through heat loss turbulence. In this study, temperature measurements were taken at a single location in the surface water of each pond and those temperatures were assumed to be consistent throughout the pond depth. As a result of the singular temperature measurement, calculated buoyancy flux was positive during any 12-hour interval with a net increase in temperature, which occurred often during sampling in the daytime, indicating lack of convection in the ponds ($w^* = 0$). However, expected in these low-wind systems, convection dominates over wind speed ($u^*/w^* < 0.75$) in sampling intervals with a net decrease in temperature of the water, indicating energy flux out of the pond. This result is consistent with previous findings that convection dominates over wind speed in small, low-wind systems (Read et al. 2012), and should be further investigated.

Previous research has noted strong diurnal variation of k_{600} in wetlands as a result of the dominance of thermal convection, with a higher gas transfer velocity overnight as a result of low-wind and heat loss in the aqueous boundary layer (MacIntyre et al. 2010, Poindexter and Variano 2013). This study found no significant difference between k_{600} during periods of cooling ($w^* > 0$) versus heating ($w^* = 0$), or between night and day. This may be due to the small sample size (n=32), or because we only sampled during the day (8 a.m. to 8 p.m.), and therefore did not pick up on overnight fluctuations in temperature. The results of this study indicate that convection plays an important role in gas exchange dynamics in small ponds, and future studies should investigate the role of convection overnight.

We were also interested in investigating how the k_{600} values for the four ponds fall into the existing body of research on gas exchange in larger bodies of water. Drawing from results from a study that determined gas transfer velocities in 40 temperate lakes (Read et al. 2012), lake surface areas were binned into seven $\log_{10}$ classes (Table 7). Taking the mean k_{600} within surface area classes takes into account the differing effects wind has on k_{600} based on surface area. Larger lakes tend to have less sheltering from wind, allowing a larger fetch over which turbulence can develop, resulting in a lower k_{600} in smaller bodies of water (Raymond et al. 2013).

Table 7: Average k_{600} in $\log_{10}$ binned surface areas of 40 temperate lakes as measured by Read et al. (2012), with the four ponds from this study included in the < 0.001 km^2 bin.

Surface Area (km^2)	< 0.001	0.001-0.01	0.01-0.1	0.1-1	1-10	10-100	100-1000
Average k_{600}	0.38	0.48	0.58	1.19	1.33	2.00	1.83

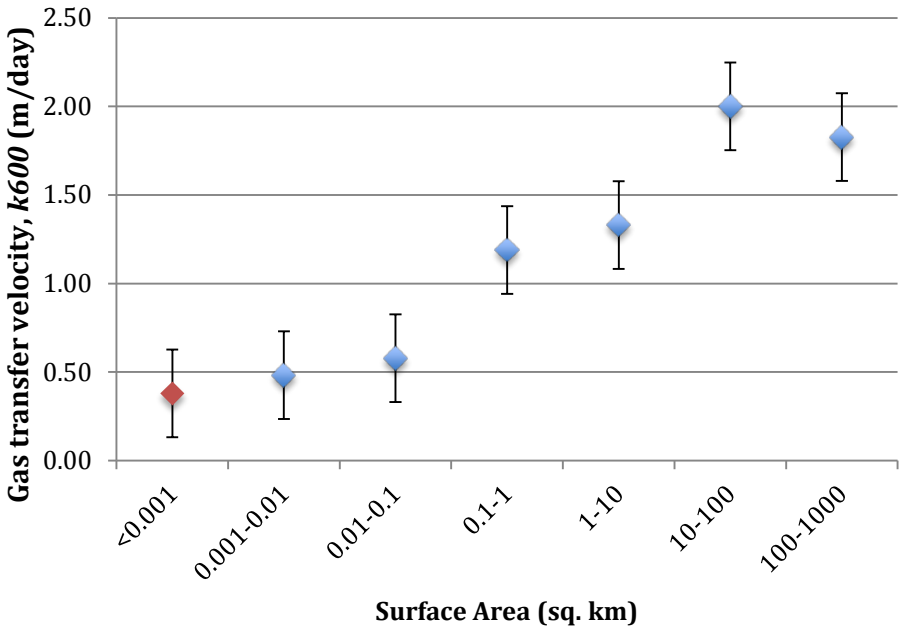

Figure 6: Plotted relationship between logarithmically binned lake or pond surface area and average gas transfer velocity in each bin, using data from Read et al. (2012). Error bars represent one standard error. Data from this study is added to the <0.001 km^2 bin, denoted in red.

This study added four systems with surface areas ~0.0002 km^2 to the < 0.001 km^2 bin, which previously contained one lake of 0.0006 km^2 with a k_{600} of 0.46 m day^{-1}. The relationship between logarithmically binned pond or lake surface area and gas transfer velocity is linear (r^2 = 0.92), with gas transfer velocity increasing as surface area increases (Figure 6). The four ponds in this study are consistent with the relationship between lake surface area and k_{600}, fitting neatly in the lower end of the existing body of data.

Previous studies have derived empirical models to estimate *k* based on wind speed in systems with moderate-to-high wind speeds (e.g., Cole and Caraco 1998, Wanninkhof 1992).

Wind speed in this study was found to have some correlation with k_{600}. However, in the small, low-wind ($U_{10,avg}$ = 0.26 m s^{-1}) systems investigated in this study, wind speed cannot be independently used as a predictive metric for k_{600} as a result of consistently low wind speeds and lack of spread between the 12-hour intervals. It should be noted, however, that while the predictive relationship between wind speed and k_{600} has been shown to break down at U < 3 m s^{-1} (e.g., Clark et al. 1994; Cole et al. 2010; Wanninkhof 1992), the two variables show a correlation down to low wind speeds. Using average wind speed measurements and k_{600} results from Read et al. 2012, the linear relationship between the two variables was found to be closely correlated (r^2 = 0.91) down to the lowest wind speeds (U < 1 m s^{-1}) (Figure 7). Adding the four ponds from this study into the graph, the k_{600} results fall roughly within the range that would be expected for the low wind speeds, but have a higher slope. Averaging all four ponds into a single data point and adding it to the Read et al. 2012 data, the results from this study align clearly within the linear fit (residual = 0.06), indicating that they fall on the low end of existing wind speed and gas transfer velocity data from larger lakes.

5 Summary

This study adds small, low-wind ponds to the existing body of research on gas transfer velocities from inland waters. These ponds are ubiquitous and may play a more significant role in the global carbon budget than previously assumed, serving as loci for terrestrial carbon cycling (Torogerson and Branco 2008). The measured k_{600} values in this study are lower than those from larger lakes with moderate-to-high wind speeds, with an overall average gas transfer velocity of 0.36 ± 0.08 m day^{-1}. Gas transfer velocity is predominantly caused by turbulence in the SML, which is controlled by wind speed and convection as well as by rain events. The ponds in this study are exposed to consistently low wind speeds as a result of canopy sheltering and have very small fetch, preventing the development of surface waves from wind. Convection, when present in the surface water, dominates over wind in creating surface turbulence. The high levels of canopy closure above the four ponds studied as well as the lack of variation across sampling prevented rainfall from having a large impact on gas transfer velocity. An accurate understanding of the carbon cycle requires the consideration of small inland waters, and the results from this study begin to fill in some of the gaps in our understanding of biogeochemistry in these systems.

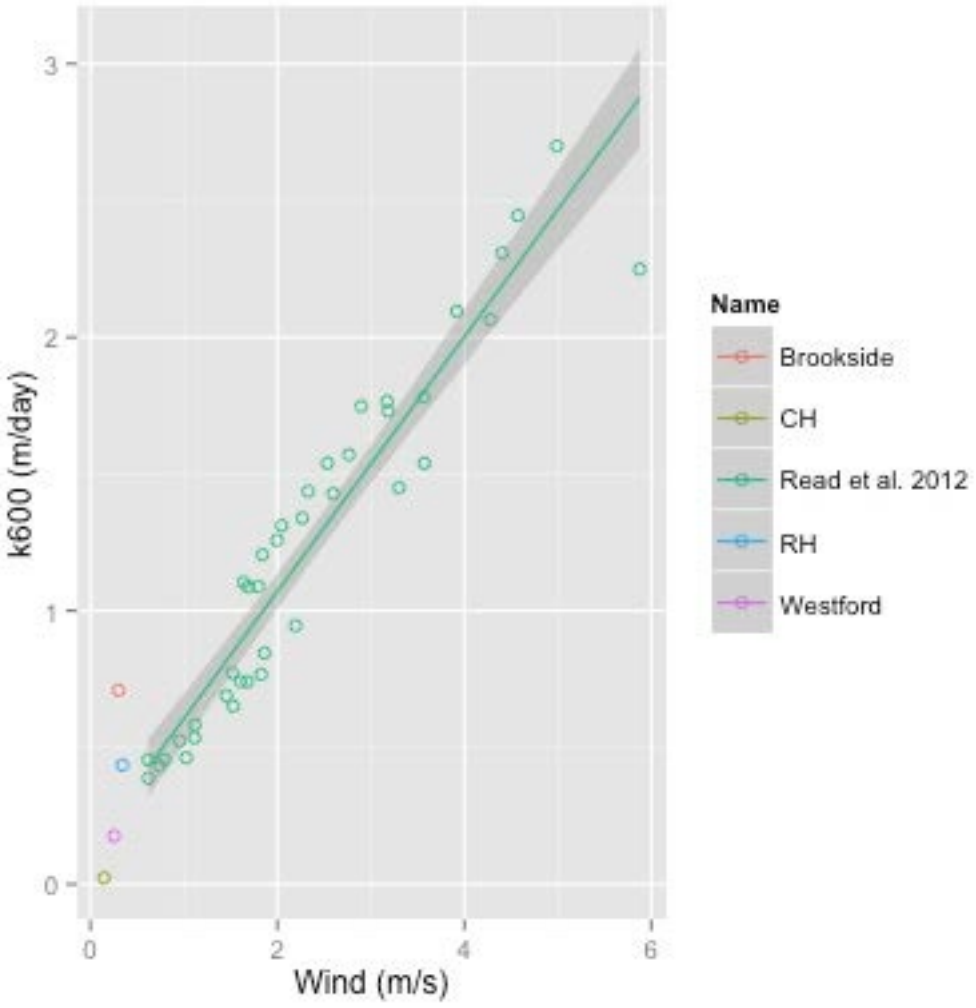

Figure 7: Relationship between average wind speed and gas transfer velocity from data in 40 temperate lakes obtained by Read et al. (2012). $r^2 = 0.91$. Line of best fit: $k_{600} = 0.46 \times U_{10,avg} + 0.16$. The four ponds from this study are added to the graph for comparison.

Acknowledgements

I would like to first thank Meredith Atwood, Ph.D. candidate at Yale F&ES, for guiding me through the literature on vernal pools and gas exchange, working with me to develop and carry out my methodology, lugging propane tanks deep into the forest, and providing invaluable help throughout the entire process. I am grateful to Dave Evans for his advising over the last four years, and Dave Bercovici for supporting me throughout my undergraduate career. Thank you to Hagit Affek, my second reader, for providing valuable insight and comments on my drafts. I would like to thank Alex Barrett, Forest Manager of Yale-Myers Forest, and the entire 2013 Forest Crew for supporting and helping me throughout my fieldwork. I would have been unable to complete this project without the help of Helmut Ernstberger, who taught me to use the KGL gas chromatography machine. Finally, I am grateful to my adviser Pete Raymond for his direction and encouragement, and for sharing his wealth of knowledge with me over the past year.

6 References

Atwood, Meredith. (2012). Dissertation Research, Unpublished.

Bridgham, S. D., Cadillo-Quiroz, H., Keller, J. K., & Zhuang, Q. (2013). Methane emissions from wetlands: biogeochemical, microbial, and modeling perspectives from local to global scales. *Global change biology*, *19*(5), 1325–46.

Brooks, R. T. 2005. A review of basin morphology and pool hydrology of isolated ponded wetlands: implications for seasonal forest pools of the northeastern United States. *Wetlands Ecology and Management* 13:335-348.

Clark, J., Wanninkhof, R., Schlosser, P., and Simpson, H. (1994). Gas exchange rates in the tidal Hudson River using a dual tracer technique. *Tellus B*, *46B*, 274–285.

Cole, J. J., Bade, D. L., Bastviken, D., Pace, M. L., and Van de Bogert, M. (2010). Multiple approaches to estimating air-water gas exchange in small lakes. *Limnology and Oceanography: Methods*, *8*, 285–293.

Cole, Jonathon and Caraco, Nina. (1998). Atmospheric Exchange of Carbon Dioxide in a Low-Wind Oligotrophic Lake Measured by the Addition of SF6. *Limnology and Oceanography* 43: 647-656.

Cole, J. J., Pace, M. L., Carpenter, S. R., & Kitchell, J. F. (2000). Persistence of net heterotrophy in lakes during nutrient addition and food web manipulations. *American Society of Limnology and Oceanography*, *45*(8), 1718–1730.

Cole, J. J., Prairie, Y. T., Caraco, N. F., McDowell, W. H., Tranvik, L. J., Striegl, R. G., Duarte, D. M., Kortelainen, P., Downing, J. A., Middelburg, J. J., Melack, J. (2007). Plumbing the Global Carbon Cycle: Integrating Inland Waters into the Terrestrial Carbon Budget. *Ecosystems*, *10*(1), 172–185.

Crusius, J., & Wanninkhof, R. (2013). Gas transfer velocities measured at low wind speed over a lake. *Limnology and Oceanography*, *48*(3), 1010–1017.

Genereux, D. P., & Hemond, H. F. (1992). Determination of Gas Exchange Rate Constants for a Small Streamon Walker Branch Watershed, Tennessee. *Water Resources Research*, *28*(9), 2365–2374.

Downing, J. A., Prairie, Y. T., Cole, J. J., Duarte, C. M., Tranvik, L. J., Striegl, R. G., McDowell, W. H., Kortelainen, P., Caraco, N. F., Melack, J. M. (2006). The global abundance and size distribution of lakes, ponds, and impoundments. *Limnology and Oceanography*, *51*(5), 2388–2397.

Ho, D., Bliven, L., Wanninkhof, R., and Schlosser, P. (1997). The effect of rain on air-water gas exchange. *Tellus B*, *49B*, 149–158.

Jähne, B., and Münnich, K. (1987). On the Parameters Influencing Air-Water Gas Exchange. *Journal of Geophysical Research*, *92*(C2), 1937–1949.

Jin, H-S., Ramsey, J.B., and White, D.S. (2008). Reaeration coefficients in a small lentic ecosystem using the propane injection method. *Nabs Annual Meeting*.

Jonas, T., Stips, A., Eugster, W., & Wuest, A. (2003). Observations of a quasi shear-free lacustrine convective boundary layer: Stratification and its implications on turbulence. *Journal of Geophysical Research*, *108*(C10).

Kelly, C. a., Fee, E., Ramlal, P. S., Rudd, J. W. M., Hesslein, R. H., Anema, C., & Schindler, E. U. (2001). Natural variability of carbon dioxide and net epilimnetic production in the surface waters of boreal lakes of different sizes. *Limnology and Oceanography*, *46*(5), 1054–1064.

Liss, P., & Slater, P. (1974). Flux of Gases across the Air-Sea Interface. *Nature*, *247*, 181–184.

MacIntyre, S., Jonsson, A., Jansson, M., Aberg, J., Turney, D. E., & Miller, S. D. (2010). Buoyancy flux, turbulence, and the gas transfer coefficient in a stratified lake. *Geophysical Research Letters*, *37*.

MacIntyre, S., Wanninkhof, R., & Chanton, J. (1995). Trace gas exchange across the air-water interface in freshwater and coastal marine environments. *Biogenic trace gases: Measuring emissions from soil and water*, 52–97.

Markfort, C. D., Perez, A. L. S., Thill, J. W., Jaster, D. a., Porté-Agel, F., & Stefan, H. G. (2010). Wind sheltering of a lake by a tree canopy or bluff topography. *Water Resources Research*, *46*.

Matthews, C. J. D., St Louis, V. L., and Hesslein, R. H. (2003). Comparison of three techniques used to measure diffusive gas exchange from sheltered aquatic surfaces. *Environmental Science & Technology*, *37*(4), 772–80.

Mohebbi, V., Naderifar, a., Behbahani, R. M., & Moshfeghian, M. (2012). Determination of Henry's law constant of light hydrocarbon gases at low temperatures. *The Journal of Chemical Thermodynamics*, *51*, 8–11.

Poindexter, C. M., and Variano, E. A. (2013). Gas exchange in wetlands with emergent vegetation: The effects of wind and thermal convection at the air-water interface. *Journal of Geophysical Research: Biogeosciences*, Unpublished.

Raymond, P., Bauer, J., and Cole, J. (2000). Atmospheric CO_2 evasion, dissolved inorganic carbon production, and net heterotrophy in the York River estuary. *Limnology and Oceanography*, *45*(8), 1707–1717.

Raymond, P. A., Caraco, N. F., & Cole, J. J. (1997). Carbon Dioxide Concentration and Atmospheric Flux in the Hudson River. *Estuaries*, *20*(2), 381–390.

Raymond, P. A., Hartmann, J., Lauerwald, R., Sobek, S., McDonald, C., Hoover, M., Butman, D., Striegl, R., Mayorga, E., Humborg, C., Kortelainen, P, Dürr, H., Meybeck, M., Ciais, P., and Guth, P. (2013). Global carbon dioxide emissions from inland waters. *Nature*, *503*(7476), 355–359.

Read, J. S., Hamilton, D. P., Desai, A. R., Rose, K. C., MacIntyre, S., Lenters, J. D., Smyth, R. L., Hanson, P. C., Cole, J. J., Staehr, P. A., Rusak, J. A., Pierson, D. C., Brookes, J. D., Laas, A, and Wu, C. H. (2012). Lake-size dependency of wind shear and convection as controls on gas exchange. *Geophysical Research Letters*, *39*(9).

Rubbo, M., J. Cole, and J. Kiesecker. (2006). Terrestrial subsidies of organic carbon support net ecosystem production in temporary forest ponds: evidence from an ecosystem experiment. *Ecosystems* 9: 1170-1176.

Torgersen, T., & Branco, B. (2008). Carbon and oxygen fluxes from a small pond to the atmosphere: Temporal variability and the CO 2 /O 2 imbalance. *Water Resources Research*, *44*(2).

Wanninkhof, R. (1992). Relationship Between Wind Speed and Gas Exchange Over the Ocean. *Journal of Geophysical Research: Oceans 97*(92): 7373–7382.

Wanninkhof, R., Ledwell, J. R., & Broecker, W. S. (1985). Gas Exchange-Wind Speed Relation Measured with Sulfur Hexafluoride on a Lake. *Science*, *227*(4691), 1224–1226.

Wanninkhof, R., Ledwell, J. R., Broecker, W. S., and Hamilton, M. (1987). Gas exchange on Mono Lake and Crowley Lake, California. *Journal of Geophysical Research*, *92*(C13), 567-580

Wanninkhof, R., & Knox, M. (1996). Chemical enhancement of CO2 exchange in natural waters. *Limnology and Oceanography*, *41*(4), 689–697.

Whalen, S.C. (2005). Biogeochemistry of Methane Exchange Between Natural Wetlands and the Atmosphere. *Environmental Engineering Science*: 22: 73-94.

Appendix A: Data Tables

Table A1: Datalogger observations, averaged over each 12-hour sampling interval.

Date	Pond	k_{600} (m day^{-1})	Avg. Water Temp. (°C)	Max. Water Temp. (°C)	Avg. Air Temp (°C)	Avg. Wind (m s^{-1})	Max. Wind (m s^{-1})	Total Rain (mm)	Avg. PAR (µmol/m^2/s)	Day/ Night
5/28/13	Westford	1.81	13.61	13.84	17.31	0.45	2.44	0	4169.04	Day
5/29/13	Westford	2.29	14.26	15.55	19.06	0.39	2.42	2.03	36144.03	Day
5/30/13	Westford	0.03	15.96	16.67	25.11	0.47	2.72	0	44099.81	Day
5/31/13	Westford	1.16	17.94	18.57	28.10	0.48	3.05	0	41963.16	Day
6/1/13	Westford	0.67	19.26	27.48	27.62	0.60	3.93	0.25	38646.92	Day
6/11/13	Brookside	2.55	12.01	12.39	18.60	0.26	1.77	17.53	684.99	Day
6/12/13	Brookside	4.52	11.42	11.59	16.69	0.56	4.3	0.51	4664.71	Day
6/13/13	Brookside	0.89	10.68	10.76	12.77	0.26	1.99	12.19	1018.78	Day
6/14/13	Brookside	3.29	10.22	10.34	14.43	0.36	2.3	1.02	4693.58	Day
6/15/13	Brookside	-0.50	10.03	10.16	18.05	0.45	2.32	0	9824.08	Day
6/18/13	CH	2.98	14.46	14.85	17.83	0.50	2.36	12.96	2072.73	Day
6/19/13	CH	5.04	13.91	14.24	18.05	0.51	2.19	0	13190.92	Day
6/20/13	CH	-0.79	13.33	14.06	19.61	0.39	3.32	0	14715.18	Day
6/21/13	CH	-2.56	13.80	14.36	21.45	0.38	1.81	0	9159.87	Day
6/22/13	CH	-0.84	14.87	26.02	21.80	0.45	1.7	2.79	10218.97	Day
6/26/13	RH	4.35	18.57	18.62	22.70	0.31	2.08	2.03	3872.75	Day
6/27/13	RH	1.59	19.12	20.74	19.90	0.21	1.16	1.02	6051.07	Day
6/28/13	RH	2.59	23.94	24.48	22.05	0.37	3.53	0.76	22435.36	Day
6/29/13	RH	2.20	25.15	27.43	22.73	0.40	2.96	0.25	28115.79	Day
6/30/13	RH	-11.27	23.03	23.52	24.39	0.34	2.48	0	30202.60	Day
5/28/13	Westford	0.17	13.61	13.88	13.47	0.29	1.74	2.54	316.81	Night
5/29/13	Westford	0.08	15.86	17.16	16.91	0.29	3.29	16.00	1554.11	Night
5/30/13	Westford	0.19	17.23	17.55	20.21	0.17	1.15	0	1289.98	Night
5/31/13	Westford	0.73	19.13	19.41	19.57	0.29	0.86	0	1376.63	Night
6/11/13	Brookside	-0.07	11.95	12.33	14.14	0.27	1.97	0	135.14	Night

6/12/13	Brookside	1.11	11.05	11.31	10.47	0.17	0.86	0	149.41	Night
6/13/13	Brookside	0.29	10.58	10.75	10.49	0.40	2.34	29.72	97.78	Night
6/14/13	Brookside	0.12	10.01	10.14	11.43	0.18	0.94	0	135.55	Night
6/18/13	CH	-0.07	14.14	14.52	13.08	0.35	1.63	1.78	137.21	Night
6/19/13	CH	0.15	13.45	14.01	10.89	0.17	0.83	0	133.09	Night
6/20/13	CH	0.09	13.68	13.87	13.55	0.20	0.81	0	137.43	Night
6/21/13	CH	-0.30	14.29	14.43	15.89	0.17	0.59	0	174.61	Night
6/26/13	RH	0.85	18.55	18.57	19.85	0.21	1.1	0	279.89	Night
6/27/13	RH	0.18	22.57	24.28	19.04	0.28	1.47	5.84	241.90	Night
6/28/13	RH	0.10	24.62	26.41	20.44	0.18	0.93	0	608.92	Night
6/29/13	RH	0.22	23.04	23.38	20.37	0.15	0.7	0	628.14	Night

Table A2: Derived values over each 12-hour sampling interval.

Date	Pond	k_{600} (m day^{-1})	$U_{10,avg}$ (m s^{-1})	Q (W m^{-2})	β (m^2 s^{-3})	u^*	w^*	u^*/w^*	Day/Night
5/28/13	Westford	0.44	0.55	5122.51	8.22E-07	1.79E-03	0.00E+00	Inf	Day
5/29/13	Westford	0.55	0.37	7354.39	1.13E-06	1.52E-03	0.00E+00	Inf	Day
5/30/13	Westford	0.01	0.58	4254.96	6.16E-07	1.81E-03	0.00E+00	Inf	Day
5/31/13	Westford	0.28	0.61	3689.79	5.28E-07	1.85E-03	0.00E+00	Inf	Day
6/11/13	Brookside	0.61	0.14	6485.25	1.05E-06	9.87E-04	0.00E+00	Inf	Day
6/12/13	Brookside	1.08	0.82	-1061.22	-1.77E-07	2.13E-03	2.12E-02	1.00E-01	Day
6/13/13	Brookside	0.21	0.14	-187.05	-3.14E-08	1.01E-03	1.27E-02	7.94E-02	Day
6/14/13	Brookside	0.79	0.30	-702.66	-1.19E-07	1.39E-03	1.93E-02	7.20E-02	Day
6/18/13	CH	0.72	0.63	4944.90	7.98E-07	1.91E-03	0.00E+00	Inf	Day
6/19/13	CH	1.21	0.66	2947.68	4.63E-07	1.93E-03	0.00E+00	Inf	Day
6/20/13	CH	-0.19	0.34	7856.39	1.26E-06	1.46E-03	0.00E+00	Inf	Day
6/21/13	CH	-0.61	0.33	6932.10	1.11E-06	1.43E-03	0.00E+00	Inf	Day
6/26/13	RH	1.04	0.18	173.02	2.45E-08	1.12E-03	0.00E+00	Inf	Day
6/27/13	RH	0.38	0.07	12798.63	2.06E-06	7.63E-04	0.00E+00	Inf	Day
6/28/13	RH	0.62	0.27	-2119.11	-3.63E-07	1.32E-03	2.67E-02	4.95E-02	Day

6/29/13	RH	0.53	0.33	-25435.73	-4.14E-06	1.43E-03	5.34E-02	2.68E-02	Day
5/28/13	Westford	0.17	0.19	-1632.87	-2.65E-07	1.14E-03	1.89E-02	6.04E-02	Night
5/29/13	Westford	0.08	0.19	-2191.56	-3.57E-07	1.13E-03	1.04E-02	1.09E-01	Night
5/30/13	Westford	0.19	0.06	3019.87	4.86E-07	6.87E-04	0.00E+00	Inf	Night
5/31/13	Westford	0.73	0.19	955.39	1.52E-07	1.15E-03	0.00E+00	Inf	Night
6/11/13	Brookside	-0.07	0.15	-3463.98	-5.60E-07	1.03E-03	2.92E-02	3.51E-02	Night
6/12/13	Brookside	1.11	0.05	-2483.15	-4.02E-07	6.61E-04	2.60E-02	2.54E-02	Night
6/13/13	Brookside	0.29	0.37	-1505.54	-2.44E-07	1.54E-03	2.29E-02	6.73E-02	Night
6/14/13	Brookside	0.12	0.06	-1024.78	-1.66E-07	6.98E-04	1.88E-02	3.71E-02	Night
6/18/13	CH	-0.07	0.27	-3462.71	-5.60E-07	1.33E-03	3.03E-02	4.39E-02	Night
6/19/13	CH	0.15	0.05	-7616.96	-1.23E-06	6.53E-04	3.67E-02	1.78E-02	Night
6/20/13	CH	0.09	0.08	-3122.51	-5.05E-07	7.76E-04	2.74E-02	2.84E-02	Night
6/21/13	CH	-0.30	0.05	-1943.77	-3.15E-07	6.60E-04	2.30E-02	2.86E-02	Night
6/26/13	RH	0.85	0.08	141.04	2.26E-08	7.71E-04	0.00E+00	Inf	Night
6/27/13	RH	0.18	0.14	24279.27	3.93E-06	1.01E-03	0.00E+00	Inf	Night
6/28/13	RH	0.10	0.05	18962.12	3.07E-06	6.70E-04	0.00E+00	Inf	Night
6/29/13	RH	0.22	0.03	993.01	1.60E-07	5.35E-04	3.17E-03	1.69E-01	Night

Table A3: Measured and derived values for each 2-3 hour sampling interval.

Pond	Date	Time	Water Temp. (°C)	Air Temp. (°C)	Rain (mm)	U_{avg} (m s^{-1})	k_{600} (m day^{-1})	Depth	Net Surface Energy Flux, Q (W $m^{-2)}$
Westford	28-May	16:00	13.34	19.35	0	0.32	NA	30.99	NA
Westford	28-May	17:30	13.5	18.35	0	0.64	-6.32	30.99	13823223.60
Westford	28-May	19:00	13.71	16.19	0	0.46	9.94	30.99	18142980.97
Westford	29-May	8:00	13.38	13.56	0	0.28	0.65	30.99	-3289661.38
Westford	29-May	10:00	13.45	14.3	1.27	0.35	4.17	30.99	4535745.24
Westford	29-May	12:00	13.79	16.06	0	0.30	-0.80	30.99	22030762.61
Westford	29-May	14:00	14.04	21.14	0	0.44	5.52	30.99	16199090.15
Westford	29-May	16:00	14.73	23.97	0.508	0.52	2.24	30.99	44709488.82

Westford	29-May	18:00	15.18	22.31	0	0.39	1.10	30.99	29158362.27
Westford	29-May	20:00	15.55	19.87	0	0.29	1.20	30.99	23974653.42
Westford	30-May	8:00	15.49	18.07	0	0.15	0.33	30.99	-647963.61
Westford	30-May	11:00	15.54	23.65	0	0.53	-2.29	30.99	2159878.69
Westford	30-May	14:00	15.84	28.19	0	0.64	2.90	30.99	12959272.12
Westford	30-May	17:00	16.38	27.44	0	0.62	1.26	30.99	23326689.82
Westford	30-May	20:00	16.67	23.69	0	0.15	-3.78	30.99	12527296.38
Westford	31-May	8:00	17.51	21.32	0	0.10	0.81	30.99	9071490.48
Westford	31-May	11:00	17.58	28.1	0	0.36	0.74	30.99	3023830.16
Westford	31-May	14:00	17.84	31.32	0	0.56	0.35	30.99	11231369.17
Westford	31-May	17:00	18.33	28.99	0	0.61	1.95	30.99	21166811.13
Westford	31-May	20:00	18.57	24.32	0	0.37	1.62	30.99	10367417.70
Brookside	11-Jun	16:00	11.83	19.1	0	0.12	NA	46.15	17111580.55
Brookside	11-Jun	18:00	12.13	18.31	0.508	0.21	-0.65	46.15	28942435.94
Brookside	11-Jun	20:00	12.38	17.48	0	0.24	5.76	46.15	24118696.61
Brookside	12-Jun	8:00	11.54	13.93	0	0.42	-0.31	46.15	-13506470.10
Brookside	12-Jun	10:00	11.51	15.89	0	0.57	18.43	46.15	-2894243.59
Brookside	12-Jun	12:00	11.48	15.9	0	0.44	-1.02	46.15	-2894243.59
Brookside	12-Jun	14:00	11.44	17.86	0	0.70	6.24	46.15	-3858991.46
Brookside	12-Jun	17:00	11.46	18.08	0	0.55	6.72	46.15	1286330.49
Brookside	12-Jun	20:00	11.26	15.72	0	0.19	-3.44	46.15	-12863304.86
Brookside	13-Jun	8:00	10.76	11.38	0	0.10	4.61	46.15	-8039565.54
Brookside	13-Jun	11:00	10.65	13.78	0	0.15	-9.67	46.15	-7074817.67
Brookside	13-Jun	14:00	10.71	13.09	0.762	0.20	6.99	46.15	3858991.46
Brookside	13-Jun	17:00	10.66	12.53	0	0.33	3.32	46.15	-3215826.22
Brookside	14-Jun	20:00	10.7	11.18	0.508	0.34	4.88	46.15	2572660.97
Brookside	14-Jun	8:00	10.34	11.07	0.508	0.39	4.98	46.15	-5788487.19
Brookside	14-Jun	11:00	10.23	11.96	0	0.42	-3.09	46.15	-7074817.67
Brookside	14-Jun	14:00	10.22	15.36	0	0.45	10.77	46.15	-643165.24
Brookside	14-Jun	17:00	10.17	17.46	0	0.40	-8.52	46.15	-3215826.22
CH	18-Jun	15:00	14.24	22.42	0	0.39	NA	47.94	-11175573.37

CH	18-Jun	17:00	14.77	16	0	0.59	-0.58	47.94	53118296.54
CH	18-Jun	19:00	14.6	15.38	0	0.41	6.55	47.94	-17037944.17
CH	19-Jun	8:00	13.72	12.86	0	0.51	-0.27	47.94	-13568679.52
CH	19-Jun	10:00	13.56	16.07	0	0.56	1.44	47.94	-16035712.16
CH	19-Jun	12:00	13.52	18.68	0	0.62	11.21	47.94	-4008928.04
CH	19-Jun	14:00	14.23	20.31	0	0.65	-4.35	47.94	71158472.72
CH	19-Jun	17:00	14.16	19.8	0	0.51	6.53	47.94	-4677082.71
CH	19-Jun	20:00	14.01	15.28	0	0.15	9.20	47.94	-10022320.10
CH	20-Jun	8:00	12.64	11.94	0	0.16	0.63	47.94	-22884297.57
CH	20-Jun	11:00	12.58	19.17	0	0.44	7.80	47.94	-4008928.04
CH	20-Jun	14:00	13.85	22.6	0	0.56	-23.36	47.94	84855643.53
CH	20-Jun	17:00	13.79	21.43	0	0.34	8.55	47.94	-4008928.04
CH	20-Jun	20:00	13.83	18.5	0	0.22	10.45	47.94	2672618.69
CH	21-Jun	8:00	13.26	14.84	0	0.34	0.38	47.94	-9521204.10
CH	21-Jun	11:00	13.3	21.16	0	0.42	-4.64	47.94	2672618.69
CH	21-Jun	14:00	13.97	24.66	0	0.58	-12.83	47.94	44766363.12
CH	21-Jun	17:00	14.22	22.34	0	0.26	2.56	47.94	16703866.84
CH	21-Jun	20:00	14.36	20.18	0	0.24	7.26	47.94	9354165.43
RH	26-Jun	16:00	18.6	24.1	0	0.46	NA	55.63	-12975784.28
RH	26-Jun	18:00	18.58	21.7	1.27	0.46	4.68	55.63	-2325848.13
RH	26-Jun	20:00	18.56	21.38	0	0.09	4.01	55.63	-2325848.12
RH	27-Jun	8:00	18.58	19.54	0	0.19	3.53	55.63	387641.35
RH	27-Jun	10:00	18.56	19.61	0	0.19	3.02	55.63	-2325848.12
RH	27-Jun	12:00	18.57	19.63	0	0.21	0.94	55.63	1162924.06
RH	27-Jun	14:00	18.59	19.78	0	0.19	0.04	55.63	2325848.12
RH	27-Jun	17:00	18.81	20.56	0	0.32	2.20	55.63	17056219.58
RH	27-Jun	20:00	20.63	20.09	0	0.11	2.11	55.63	141101452.92
RH	28-Jun	8:00	23.88	20	0	0.25	0.75	55.63	62991720.05
RH	28-Jun	11:00	24.12	22.8	0	0.47	4.64	55.63	18606785.00
RH	28-Jun	14:00	24.22	23.22	0	0.35	3.88	55.63	7752827.08
RH	28-Jun	17:00	23.79	22.24	0	0.31	0.83	55.63	-33337156.46

RH	28-Jun	20:00	23.51	21.55	0	0.27	1.26	55.63	-21707915.83
RH	29-Jun	8:00	26.16	20.8	0	0.22	0.43	55.63	51362479.43
RH	29-Jun	11:00	26.53	21.52	0	0.34	2.95	55.63	28685460.21
RH	29-Jun	14:00	26.26	24.22	0	0.58	2.90	55.63	-20932633.13
RH	29-Jun	17:00	23.73	23.83	0	0.44	0.63	55.63	-196146525.21
RH	29-Jun	20:00	23.05	21.39	0	0.17	2.74	55.63	-52719224.17

Appendix B: R Code for Statistical Analysis

Analysis of the Relationship of k_{600} with Environmental Variables and Pond-Specific Parameters

```
> #Multiple Regression for environmental variables
> k.daynight$nearrain<-c(0,0,1,0,1,0,1,1,0,0,0,0,0,0,0,0,1,0,0,1,0,1,0,1,0,0,0,0,0,0,0)
> fit2<-lm(k.daynight$k600~k.daynight$U10+k.daynight$nearrain+k.daynight$depth+k.daynight$SA)
> summary(fit2)

Call:
lm(formula = k.daynight$k600 ~ k.daynight$U10 + k.daynight$nearrain +
    k.daynight$depth + k.daynight$SA)

Residuals:
    Min      1Q  Median      3Q     Max
-0.8346 -0.2299 -0.0428  0.2015  0.7280

Coefficients:
                  Estimate Std. Error t value Pr(>|t|)
(Intercept)       -3.564353   1.167657  -3.053  0.00505 **
k.daynight$U10     0.794011   0.321305   2.471  0.02007 *
k.daynight$nearrain -0.354359   0.167218  -2.119  0.04342 *
k.daynight$depth    0.018821   0.008394   2.242  0.03335 *
k.daynight$SA       0.014482   0.004713   3.072  0.00481 **
---
Signif. codes:  0 ‘***’ 0.001 ‘**’ 0.01 ‘*’ 0.05 ‘.’ 0.1 ‘ ’ 1
```

```
Residual standard error: 0.3685 on 27 degrees of freedom
Multiple R-squared:  0.3691,  Adjusted R-squared:  0.2757
F-statistic: 3.949 on 4 and 27 DF,  p-value: 0.01192
> #ANOVA for diff between surface areas
> anova.SA<-aov(k.daynight$k600~k.daynight$SA,data=k.daynight)
> summary(anova.SA)
             Df Sum Sq Mean Sq F value Pr(>F)
k.daynight$SA  1  0.395  0.3952   2.189  0.149
Residuals     30  5.415  0.1805
> #ANOVA for diff between depths
> anova.depth<-aov(k.daynight$k600~k.daynight$depth,data=k.daynight)
> summary(anova.depth)
               Df Sum Sq Mean Sq F value Pr(>F)
k.daynight$depth  1  0.068  0.0679   0.355  0.556
Residuals        30  5.743  0.1914
```

Analysis of k_{600} between days and ponds

```
> #T-test for difference night/day
> t.test(k.daynight$k600[k.daynight$DN=="Day"], k.daynight$k600[k.daynight$DN=="Night"])

        Welch Two Sample t-test

data:  k.daynight$k600[k.daynight$DN == "Day"] and k.daynight$k600[k.daynight$DN == "Night"]
t = 1.602, df = 27.933, p-value = 0.1204
alternative hypothesis: true difference in means is not equal to 0
95 percent confidence interval:
 -0.06669645  0.54519436
sample estimates:
mean of x mean of y
0.4792351 0.2399862

> #ANOVA for difference between ponds
```

```
> anova.pondsbyday<-aov(k.daynight$k600~k.daynight$pond,data=k.daynight)
> summary(anova.pondsbyday)
                Df Sum Sq Mean Sq F value Pr(>F)
k.daynight$pond  3  0.806  0.2686   1.503  0.235
Residuals       28  5.005  0.1787
```